Supporting Information. Bozec, Y.-M., K. Hock, R. A. B. Mason, M. E. Baird, C. Castro-Sanguino, S. A. Condie, M. Puotinen, A. Thompson, and P. J. Mumby. 2021. Cumulative impacts across Australia's Great Barrier Reef: a mechanistic evaluation. Ecological Monographs.

APPENDIX S1: CORAL POPULATION MODEL

General description

The model represents a mid-depth (5–10 m) reef environment and simulates with a 6-month time step the settlement, growth and mortality of coral colonies and the dynamics of patches of reef algae onto a 20 × 20 grid lattice of 1 m^2 cells. The lattice grid has a toroidal structure (i.e., wrapped around) so that every cell has continuous boundaries formed by 4 neighboring cells. Each cell can be occupied by multiple coral colonies and patches of turf and macroalgae, with corals being stylized by circular areas (cm^2). A number of cells are assigned to the class "ungrazable substrata" and prevented from coral and algal colonization. This catch-all term designates abiotic substrata (e.g., sand) and sessile organisms (e.g., sponges, seagrass) whose dynamics are not considered by the model.

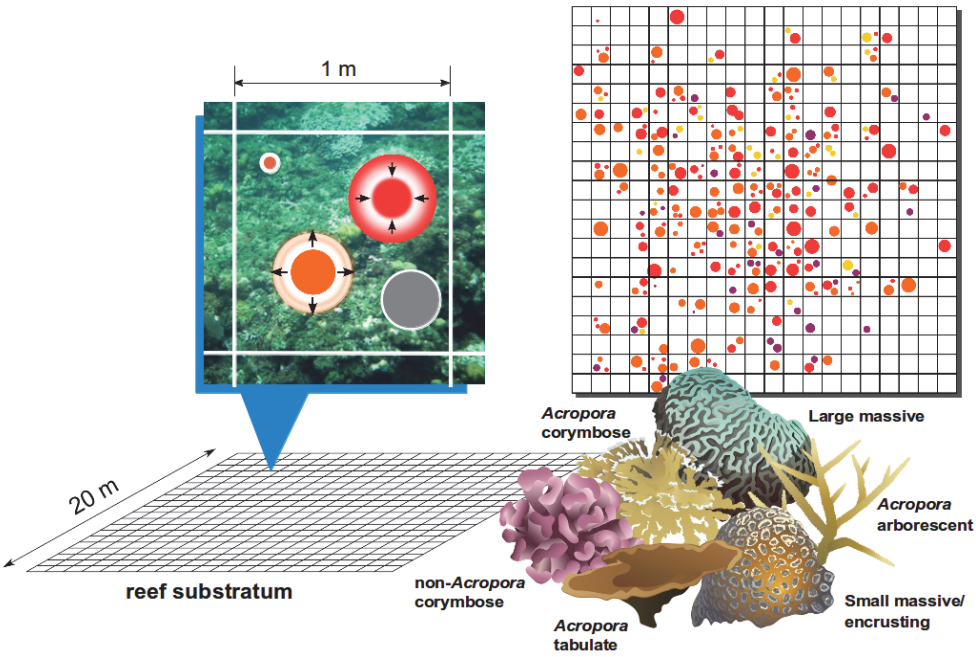

Fig. S1. Schematic representation of a modeled mid-depth (5-10m) reef environment using a 20m × 20m horizontal space on which circular coral colonies settle, grow, shrink and die. Corals are modeled by their size (planimetric area in cm^2) and belong to six functional groups: Arborescent (staghorn) acroporids; plating (tabular) acroporids; corymbose/small branching acroporids; pocilloporids and other non-acroporid corymbose corals; small massive/encrusting corals; large massive corals. Graphics of corals courtesy of the Integration and Application Network, Univ. of Maryland Center for Environ. Science.

Coral demographics, ecological interactions and the impact of acute disturbances (e.g., storms, bleaching) are explicit at colony scales and follow probabilistic rules supported by empirical observations representative of a mid-depth reef environment. Demographic rates were derived from studies mostly conducted on the Great Barrier Reef or in the wider Indo-Pacific otherwise (Appendix S2: Table S1). While this is the minimum background data required for simulating coral demographics, these rates can be refined with more specific information (i.e., different coral habitats, species composition etc.) where available. Functional responses to stressors (suspended sediment, cyclones, heat stress, predation by the Crown-of-thorns starfish) were calibrated to GBR observations, and their generalization to other reef systems may require some preliminary testing or adjustment to coral responses observed locally. Here, a spatially-realistic environmental setting (i.e., coral dispersal, suspended sediment concentrations, past cyclone tracks and thermal stress) was used to simulate credible reconstructions of observed reef dynamics across the GBR. While ReefMod-GBR enables simulation of meta-population dynamics across multiple reef grids connected by larval dispersal, the model can also be used to simulate coral demographics on a single reef grid that represents a typical reef environment, with the provision of an appropriate parameterization of external larval supply and stress exposure.

For modeling coral demographics across the GBR, six functional groups of corals were defined:

1. Arborescent (staghorn) acroporids (e.g., *Acropora muricata*, *Acropora nobilis*, *Acropora robusta*);
2. Plating acroporids (e.g., *Acropora hyacinthus*, *Acropora cytherea*);
3. Corymbose/small branching acroporids (e.g., *Acropora millepora*, *Acropora humilis*);
4. Pocilloporids/non-acroporid corymbose (e.g., *Stylophora pistillata*);
5. Small massive/submassive/encrusting corals (e.g., Lobophylliidae, favids, *Goniastrea*);
6. Large massive corals (*Porites lutea*, *Porites lobata*).

A focus on *Acropora* corals is justified as they represent the key habitat-forming species on the GBR and account for around 70% of the coral biodiversity in the Indo-Pacific region (Wallace 1999). Other model agents include patches of closely cropped algal turf (< 5mm), uncropped algal turf (> 5mm height), encrusting fleshy (i.e., *Lobophora*) and upright fleshy macroalgae. A spatially-explicit process of grazing maintains macroalgae in a cropped state, which facilitates coral settlement and growth. Grazing affects all algal groups and always results in cropped turf, on which corals can settle. Grazing is spatially limited, so that only a proportion of the grazable substrate can be efficiently grazed over 6 months. Competitive interactions between corals and macroalgae reduce the growth rate of each taxa and are the only process modeled to occur across cell boundaries (within a 4-cell von Neumann neighborhood).

At initial step, a number of cells are randomly designated as “ungrazable” until the specified cover of ungrazable substrata of the grid lattice is achieved. Ungrazable cells remain fixed

thereafter. Grazable cells are then filled at random with coral colonies of random size generated by lognormal distributions (Meesters et al. 2001) until the sum of all colony sizes matches the specified coral cover for each species at the reef (i.e., grid) scale. Finally, algal patches are created by randomly filling the remaining space in every grazable cell until the specified algal cover is reached.

All demographic rates parameters are assumed constant rather than allowed to vary probabilistically over time. This approach avoids unnecessary variation from relatively well-established demographic parameters. However, the spatial distribution of coral recruitment, natural mortality, stress-induced mortality and algal grazing are is by probabilistic rules which generates stochasticity in model simulations. Model outputs include the percent cover of each coral and algal species, the percent cover of loose coral rubble created by disturbances, and the density of coral colonies at different life stage and size.

Demographic processes

Coral fecundity. Broadcast coral spawning occurs at the beginning of the wet season (austral summer). Coral fecundity F_{coral}, expressed as the total volume of eggs per colony, is a function of colony size (Hall and Hughes 1996). :

$$F_{coral} = \exp(a + b \times \log_e x) \qquad \text{(S1)}$$

where x is the cross-sectional basal area of a colony in cm^2, and a and b are two parameters determined empirically by Hall and Hughes (1996) for some coral species (Appendix S2: Table S1). Coral colonies are considered sexually mature when their size reaches a specific threshold (Appendix 2: Table S1). Summing F_{coral} over all gravid colonies with an average egg volume of 0.1 mm^3 (for *Acropora hyacinthus*, Hall and Hughes 1996) allows estimating a number of offspring released by each coral group during the reproductive season. The number of offspring produced on a reef is further reduced according to the concentration of suspended sediment predicted during spawning events (see below Eq. S10, S11).

Coral recruitment. Corals successfully recruit to cropped turf algae (Kuffner et al. 2006, Arnold et al. 2010) at a size of 1 cm^2 (~6-month old corals). Recruitment is density-dependent and proportional to the space available for settlement. First, a potential density of settlers is determined from larval supply (number of incoming coral larvae from external and self-supply) following a Beverton-Holt function (main text Eq. 1). The actual density of 6-month-old recruits is generated at random for each cell given the potential density of settlers and the amount of settlement space in the cell (main text Eq. 2). Recruitment rates are further adjusted for each coral group based on empirical observations (Appendix 2: Table S1) and reduced by suspended sediments for the three acroporid groups (see below Eq. S12).

Coral growth. Coral colony growth is modeled as lateral extension (radius increment) at each time step (6 month). The growth rate of coral juveniles (colony diameters ≤ 4 cm) is set to

1 cm y^{-1} (Doropoulos et al. 2015, 2016), further reduced by the concentration of suspended sediments (see below Eq. S13). Adult corals grow following taxa-specific extension rates derived from literature data (Appendix 2: Table S1).

Colonization of cropped algae. Cropped turf algae is the default substratum and arises (i) when long turf and macroalgae are grazed and (ii) after all coral mortality events (Jompa and McCook 2002) except those due to macroalgal overgrowth (see coral-algal competition below).

Colonization and vegetative growth of macroalgae. The model simulates with a 1-month time step the spatial dynamics of macroalgal colonization following observations on 4–6m depth forereefs in Palau (Bozec et al. 2019). Diminutive cropped algal turf is the default substrate maintained by repeated grazing. Grazing affects all algal substrates following specified feeding preferences and all consumed algal surfaces are converted into diminutive algal turf. When a cell is left ungrazed for 1 month, diminutive algal turf converts into uncropped algal turf and defines the space available for macroalgal colonization: propagules of macroalgae then settle and grow over the uncropped turf following a logistic curve. Encrusting fleshy macroaglae can also colonize from the margins of a cell due to the horizontal expansion of the surrounding vegetation.

Macroalgal settlement occurs on uncropped turf and only in cells that are left ungrazed for 1 month. Macroalgal settlement in a cell (in cm^2) is proportional to the area of uncropped turf in that cell, with a maximum of 2.5 cm^2 per m^2 of uncropped turf (Diaz-Pulido and McCook 2004). Then, macroalgae expand horizontally over uncropped turf following two mechanisms. First, a cell can be overgrown by the surrounding vegetation of encrusting fleshy macroalgae that expands from the neighboring cells, which is calculated as follows:

$$E_{EFM} = MO_{EFM} \times EFM_{4cell} \qquad \text{(S2)}$$

where MO_{EFM} is the rate of marginal overgrowth of encrusting fleshy macroalgae per unit cover of surrounding vegetation (45 cm^2 per m^2 of uncropped turf for a 60% surrounding cover of encrusting fleshy macroalgae; De Ruyter van Steveninck and Breeman 1987) and EFM_{4cell} is the proportional cover of encrusting fleshy macroalgae calculated over the 4 neighboring cells (von Neumann neighborhood). The surrounding vegetation of encrusting fleshy macroalgae is calculated before growth for every cell, and E_{EFM} adds to the current amount of encrusting fleshy macroalgae only in those cells that escape grazing and where enough uncropped turf is available for macroalgal expansion. Uncropped turf is immediately reduced accordingly.

Second, each class of macroalgae (*MA*) expands horizontally over uncropped turf (*TURF*) following a logistic growth increment $Growth_{MA}$ (cm^2) calculated as follow:

$$Growth_{MA} = r_{MA} \times MA \times (1 - MA / (MA + TURF)) \qquad \text{(S3)}$$

where r_{MA} is the intrinsic growth rate of the corresponding macroalgal group (0.598 for encrusting fleshy macroalgae; 0.843 for upright macroalgae, Bozec et al. 2019). The sum *MA* +

TURF represents the current carrying capacity of the cell for that macroalgal group. The growth of encrusting fleshy macroalgae is processed before that of upright macroalgae. The cover of uncropped turf is reduced after each macroalgal increment.

Competition between corals. Coral growth is constrained by the space currently available in a cell, so that competition between corals occurs when the total area over which corals would potentially expand exceeds the amount of available space. In that case, free space is shared between all coral colonies proportionally to their growth potential. This reflects the ability of faster/larger colonies to overtake slower/smaller colonies, as growth potential depends both on extension rate and current colony size.

Competition between corals and cropped algae. Corals always overgrow cropped turf algae (Jompa and McCook 2002).

Competition between corals and macroalgae: reduction of coral growth rate. The growth rate of coral juveniles is set to zero if the cover of all macroalgae in the local environment formed by the focal cell and the von Neumann 4-cell neighborhood is > 80%, and reduced by 70% if total macroalgal cover lies between 40% and ≤ 80% (Box and Mumby 2007). Growth rate of larger corals is reduced by up to 90% if macroalgal cover exceeds 40% (Lirman 2001), implemented as a step function.

Competition between corals and macroalgae: macroalgal overgrowth. Limited direct overgrowth of coral by macroalgae can occur (Lirman 2001, Jompa and McCook 2002a, Nugues and Bak 2006). The macroalgal overgrowth of a living coral colony i ($O_{i \rightarrow M}$ in cm^2) results in partial mortality of the colony and is calculated as:

$$O_{C \rightarrow M} = MA_{5cells} \times P_i \times a_{MA,i} \qquad \text{(S4)}$$

where MA_{5cells} is the proportion of encrusting fleshy or erect macroalga in the local environment formed by the focal cell and the von Neumann 4-cell neighborhood, P_i is the perimeter (cm) of the coral colony i and $a_{MA,i}$ the average overgrowth (cm) of i due to the macroalga per cm length of coral edge.

Manipulative *in situ* experiments (Nugues and Bak 2006) placing *Lobophora variegata* in contact to six Caribbean coral species found that only one coral (*Agaricia agaricites*) suffered important tissue loss after one year: on average ~12 cm^2 of tissue area lost across a ~7 cm length of coral edge. This translates to $a_{L,i}$ = 0.86 cm^2 per cm length of coral edge over 6 months. Area lost averaged ~0.11 cm^2 per 6 month for the other species. *In situ* experiments on the GBR also showed that *Lobophora* can cause tissue mortality on the branching coral *Porites cylindrica* (Jompa and McCook 2002a,b). Hence, the ability of *Lobophora* to directly overgrow corals is highly variable and without specific information on the competitive abilities for the six modeled coral groups, values of $a_{L,i}$ for Pacific corals were set to a conservative value of 0.11 cm^2 per 6 month, corresponding to the less vulnerable species of Nugues and Bak (2006)'s experiment.

Lirman (2001) found no direct overgrowth of brooders by the erect macroalga *Dictyota* but an overgrowth of 0.25 – 0.43 $cm^2\ month^{-1}$ per cm length of coral edge on the coral spawner *Orbicella faveolata*. The lowest value of this range (no herbivory exclusion) translates to $a_{D,i}$ = 1.5 cm for a 6 month time step and was applied to all corals except for pocilloporids (brooders).

Competition between corals and macroalgae: effect of corals on macroalgae. Corals can inhibit the growth of macroalgae (De Ruyter van Steveninck et al. 1988, Jompa and McCook 2002b) although the responsible mechanisms for this inhibition (i.e., physical contact vs. allelopathy) are not clearly established (Jompa and McCook 2002b). The probability with which macroalgae spread vegetatively over cropped algae, $P_{A \rightarrow M}$, is reduced by 25% when at least 50% of the local von Neumann neighborhood includes coral (De Ruyter van Steveninck et al. 1988):

$$P_{A \rightarrow M} = 0.75 \times MA_{5cells}\text{ , if } C_{5cells} \geq 0.5 \qquad \text{(S5)}$$

$$P_{A \rightarrow M} = MA_{5cells}\text{ , if } C_{5cells} < 0.5 \qquad \text{(S6)}$$

where C_{5cells} is the proportion of corals in the focal cell and the 4-cell von Neumann neighborhood.

Background (chronic) whole-colony mortality of juveniles. Incidence of mortality in juvenile corals (diameter ≤4 cm, equivalent to an area of live cover <13 cm^2) is set to 0.2 y^{-1} as recorded for *Acropora* spp. on a reef slope at Heron Island (Doropoulos et al. 2015). This level of mortality is essentially due to corallivory (e.g., butterflyfish; Lenihan et al. 2011, Doropoulos et al. 2016) and occurs at every time step in addition to macroalgal overgrowth and mortality caused by acute disturbances.

Background (chronic) whole-colony mortality of adults. Incidence of mortality of corals between 13–250 cm^2 is set to 0.04 y^{-1} and 0.02 y^{-1} for corals above 250 cm^2 (Bythell et al. 1993, further adjusted to each coral group, see Appendix 2: Table S1). These levels of mortality occur at every time step in addition to macroalgal overgrowth and mortality caused by acute disturbances.

Background (chronic) partial-colony mortality of corals. Partial mortality is colony size-dependent, following empirical observations from Curaçao before major bleaching or hurricane disturbances (Meesters et al. 1997). State variables reported in literature were converted to dynamic variables using least squares optimization until the equilibrial state in the model matched observed data (Mumby et al. 2014) leading to the two equations below, where P_{pm} is the probability of a partial mortality event, A_{pm} is the area of tissue lost in a single event, and x is the size (planimetric area) of the coral in cm^2 before shrinkage:

$$P_{pm} = 1 - [\,(88.9 - 11.2 \times \log_e x) \,/\, 100\,] \qquad \text{(S7)}$$

$$\log_e(A_{pm} \times 100) = -2.9 + 1.59 \times \log_e x \qquad \text{(S8)}$$

The extent of tissue lost (A_{pm}) is further adjusted to each coral group following calibration with Pacific corals (Ortiz et al. 2014, see Appendix 2: Table S1). These levels of mortality occur at every time step in addition to macroalgal overgrowth and mortality caused by acute disturbances.

Herbivory. Grazing is spatially constrained (Williams et al. 2001) and is expressed as the proportion of the total reef surface efficiently maintained in a cropped state every month, which essentially represents the overall net impact of grazing resulting from the balance between continuous growth and consumption of algae at the reef scale (Mumby et al. 2007, Bozec et al. 2019). This net grazing impact (*GI*) can either be fixed, follow a stochastic stationary process or coupled with expected temporal variations in herbivorous fish abundance (Bozec et al. 2016). At each monthly time step *t*, *GI*(*t*) is adjusted to the reef surface currently available for grazing:

$$GA(t) = GI(t) \ / \ (1 - UNGRAZ(t)) \qquad \text{(S9)}$$

where *UNGRAZ*(*t*) represents the proportional area that is not available to algal colonization at time step *t* (ie, the summed cover of coral cover and ungrazable substrates). Thus, *GA*(*t*) represents the current proportion of the grazable area that is maintained in a cropped state. This essentially allows integrating the functional impact of ungrazable space, which, by reducing the grazable area of the reef, intensifies grazing on the remaining algal substrates (Williams et al. 2001). *GA*(*t*) is then converted into the equivalent algal surface (cm^2) grazed over the reef grid. Algal removal is conducted randomly across grid cells and distributed among each algal group following specified feeding preferences (Bozec et al. 2019), which are merely rules of consumption reflecting community-wide algal selectivity of fish herbivores. Considering that herbivorous fish are largely unexploited across the GBR, we set grazing to the maximum value (i.e., *GI*=1) with the implication that macroalgae and turf are maintained in a cropped state. All consumed algal surfaces are converted into cropped algal turf for the next model iteration.

Impacts of suspended sediments on coral larvae, recruits and juveniles. Using dose-response experiments, Humanes et al. (2017a) assessed the effects of suspended sediment concentrations (*SSC)*, temperature and nutrient concentrations on the rate of fertilization of the broadcast spawning coral *Acropora tenuis*. Increasing *SSC* (5 levels: 0, 5, 10, 30, 100 mg/L) significantly and negatively affected the proportion of fertilized eggs, whereas nutrients and temperature had no or negligible impact. From the reported data (effect of each treatment averaged over 12 replicates), a dose-response curve of fertilization success to increasing *SSC* (mg/L) can be fitted to the proportion of fertilized eggs across all nutrient treatments at ambient temperature ($R^2 = 0.88$, $n = 20$ treatments, Appendix S3: Fig. S1A):

$$FERT\% = 97.417 \times \exp(-0.010 \times SSC) \qquad \text{(S10)}$$

A second experiment exposed 8-hour-old embryos of *A. tenuis* to *SSC* treatments for 28 hours (i.e., until embryos became ciliated larvae) and measured the rates of subsequent survival and settlement (Humanes et al. 2017a). While early stress exposure did not affect survival to the settlement stage, the proportion of settled larvae was significantly influenced by all stressors,

with *SSC* having the strongest negative effect. The reported mean effects of *SSC* treatments at low and medium nutrient concentrations under ambient temperature (12 replicates for each treatment) can be combined to fit a dose-response curve of settlement success to increasing *SSC* in mg/L ($R^2 = 0.88$, $n = 20$ treatments, Appendix S3: Fig. S1A):

$$SETT\% = 99.571 - 10.637 \times \log(SSC + 1) \quad \text{(S11)}$$

In another study, Humanes et al. (2017b) assessed the survival and growth of young (< 6 month-old) recruits of *Acropora millepora*, *A. tenuis* and *Pocillopora acuta* after 40 days of exposure to increased concentrations of suspended sediments (4 levels: 0, 10, 30, 100 $mg.L^{-1}$) and nutrients. The reported mean effect of *SSC* relative to the null *SSC* treatment across all nutrient treatments (3 replicate tanks for each treatment) can be combined for the two *Acropora* species to fit a dose-response curve of survival (over 40 days) to increasing *SSC* ($R^2 = 0.89$, $n = 8$ treatments, Appendix S3: Fig. S1B):

$$SURV = 1 - 1.88e\text{-}03 \times SSC \quad \text{(S12)}$$

After conversion to daily survival rates, Eq. S12 was applied to the three acroporid groups only, since no significant effect of *SSC* was observed on the survival of *P. acuta* recruits. Practically, this amounts to reducing $D_{recruits}$ to the predicted surviving fraction.

In the same study (Humanes et al. 2017b), *SSC* was also found to reduce the growth of recruits (Appendix S3: Fig. S1C) and we assume here that a single curve fits the growth response of the three species ($R^2 = 0.79$, $n = 12$ treatments) and can be extrapolated to the growth of any coral juvenile:

$$RelG = 1 - 0.176 \times \log(SSC + 1) \quad \text{(S13)}$$

Cyclone impact on juvenile and adult corals: colony dislodgement. Storm-induced (acute) whole-colony coral mortality (i.e., dislodgement) is modeled as a function of colony size and storm strength (Mumby et al. 2007, Edwards et al. 2011). For category 5 cyclones, the probability (incidence) of whole-colony mortality P_{wcm_cyc5} was represented using a quadratic function where x is the cross-sectional basal area of the colony in cm^2 (Bythell et al. 1993, Massel and Done 1993):

$$P_{wcm\_cyc5} = -3e\text{-}07\ x^2 + 7e\text{-}04\ x + 0.0551\ \varepsilon \quad \text{(S14)}$$

Small colonies avoid dislodgement due to their low drag. Intermediate-sized corals have greater drag and are light enough to be dislodged, whereas large colonies are heavy enough to prevent dislodgement. A Gaussian-distributed noise $\varepsilon \sim (\mu = 0, \sigma = 0.1)$ adds variability to mortality predictions. For lower cyclone categories, this function is modified by lowering the peak by the predicted impacts of each storm category relative to the impacts of a category 5 cyclone (Edwards et al. 2011). These relative predicted impacts (category 1: 4.6%; category 2: 11.8%; category 3: 25.0%; category 4: 56.8%) were determined by a simple relationship between storm

intensity (wind speed), wave height, and predicted dislodgement (Madin and Connolly 2006). Details on these calculations can be found in Edwards et al. (2011).

Cyclone impact on mature corals (> 250 cm^2): partial mortality. The extent of partial mortality due to cyclones (A_{pm_cyc}) is modeled using a Gaussian distribution with mean and standard deviation dependent on storm strength (with maximum mean of 0.30 and standard deviation of 0.20 for a category 5 cyclone, reduced as above for other cyclone categories). A_{pm_cyc} represents the percentage of original colony tissue that is lost due to the cyclone and is generated at random for every single colony. If $A_{pm\_cyc} \leq 0$, there is no partial mortality. If $A_{pm\_cyc} \geq 1$, the entire colony is lost (though this is a rare event). Data come from monitoring of impact of Hurricane Mitch in Belize (Mumby et al. 2005).

Cyclone impact on coral recruits (1-60 cm^2): scouring by sand. Scouring by sand during a cyclone causes 80% whole-colony mortality in small corals (Mumby 1999).

Cyclone impact on macroalgae. Cyclones reduce the cover of macroalgae to 10% of its pre-cyclone level (Mumby et al. 2005).

Bleaching-induced whole-colony mortality. Whole-colony mortality caused by mass bleaching is a function of thermal stress (main text Eq. 3) obtained by regression of shallow (2m depth) observations of initial bleaching mortality (Hughes et al. 2018) against satellite-derived DHW (Liu et al. 2017) across the GBR during the 2016 marine heatwave. For a reef with predicted heat stress ≥ 3 °C-weeks, the incidence of bleaching mortality is generated with a random noise (Gaussian distribution of mean 0 and variance equal to the estimated error variance of the regression model). The resulting incidence of initial mortality is adjusted to each coral group (Appendix S2: Table S1) following bleaching susceptibilities reported at the taxon level by Hughes et al. (2018), and extended to 6 months by calibration with the observed 8-months changes of coral cover following the 2016 mass beaching (see details below).

We assume that bleaching on a reef does not occur if the predicted DHW < 3 °C-weeks or if the SST near that reef was likely cooled by a nearby cyclone during the same season. Assuming an adequate reservoir of deeper cool water is available, cyclones can cool SST nearby, usually 1-6 but up to 11°C (Zhang 2021). In the Caribbean, bleaching was shorter lived and less severe at sites cooled by cyclones versus those that were not (Manzello et al. 2007), and thermal stress relief from cyclones was evident across broad spatial scales over an entire season (Carrigan and Puotinen 2014).

Partial-colony mortality due to bleaching. The incidence of partial mortality due to bleaching is equal to that of whole-colony mortality. For a coral affected by partial mortality, the extent of tissue lost (Baird and Marshall 2002) is set to 40% of the colony area for small massive/submassive (observations on *Platygyra daedalea*), 20% for large massive corals (*Porites lobota*), and a minimal 5% for the three acroporid groups (*A. hyacinthus* and *A. millepora*) extended to pocilloporids due to morphological similarities (i.e., branching corals).

Calibration

Calibration of parameters of coral recruitment. Because the processes that link larval supply and the number of 6-month old recruits are largely uncertain, recruitment parameters α and β (main text Eq. 1) for corals were determined by calibration against GBR observations from offshore (mid- and outer-shelf) reefs. We simulated coral recovery on hypothetical reefs (n = 100) and adjusted these two parameters with the constraint of reproducing simultaneously two observed data sets: 1) the recovery dynamics of coral cover following extensive coral loss (Emslie et al. 2008, Fig. 2A); 2) spatial variations in the density of coral juveniles (Trapon et al. 2013, Fig. 2B). Reefs were initialized with a random coral cover generated from a normal distribution $N(\mu = 5\%, \sigma = 0.2\times\mu)$, equally distributed among all groups. Initial proportions of loose coral rubble and ungrazable substrata were generated similarly to coral cover but with a mean set to 10% and 30%, respectively. Coral connectivity and stress-induced mortality were turned off. With α = 15 settler/m^2 distributed across the six coral groups (Trapon et al. 2013, Appendix S2: Table S1) and β = 75,000 larva/m^2 (among all groups), the model achieved realistic recovery rates (from ~10% to ~60% in 6-7 years) with juvenile densities within the range of empirical observations.

Calibration of storm-induced coral mortality. The above calculations of cyclone impacts inherited from previous model parameterizations specific to Caribbean reefs (Mumby et al. 2007, 2014, Edwards et al. 2011, Bozec et al. 2015). To obtain more reliable predictions for GBR corals, cyclone-driven mortalities were calibrated with observations of storm damages from the benthic photo-transect survey database of the Australian Institute of Marine Science (AIMS) Long-Term Monitoring Program (LTMP). Coral cover data were extracted on reefs surveyed within one year of a designated storm exposure (pre- and post-disturbance), leading to the selection of 13 reefs (with 3 sites per reef) exposed to 4 cyclones: Justin (March 1997), Tessi (April 2000), Hamish (March 2009) and Yasi (February 2011). Cyclone exposure for each reef was reconstructed using the Database of Past Tropical Cyclone Tracks of the Australian Bureau of Meteorology (BoM). For each cyclone track (6-hour position of the storm center) a category of storm intensity defined on the Saffir-Simpson scale was assigned based on the reported value of maximum sustained winds converted into a 1-minute equivalent. Storm intensity experienced by a surveyed reef was estimated from its distance to the cyclone track, assuming asymmetric threshold distances of wind intensity from the storm center (Edwards et al. 2011). Because the spatial extent of wind intensity (and the resultant sea state that produces damaging waves) greatly varies with storm size and translation speed, threshold distances used to assign each cyclone category were further adjusted following spatial predictions of damaging sea state (average top 1/3 of wave heights [significant wave height – Hs] ≥ 4 m) relative to threshold distances for a given storm size (mean radius of gale force winds) as per Puotinen et al. 2016). As a result, the expected storm intensities fall within cyclone category 1 (n = 15 sites), 2 (n = 18) and 4 (n = 6). Simulations of coral damage at each LTMP site were run under the expected storm intensity to adjust the predictions of partial- and whole-colony mortality to the observed changes

in coral cover. For each surveyed site, the model was initialized with the observed pre-disturbance cover of 37 coral taxa assigned to the modeled coral groups. Multiplying by 5 the initial predictions of partial and whole-colony mortalities, further adjusted to each coral group following the response observed in the corresponding coral taxa (Appendix S2: Table S1), produced a reasonable match between the simulated and observed coral cover changes for the expected cyclone categories (main text, Fig. 2C).

Calibration of coral mortality due to bleaching. The relationship between DHW and coral mortality (main text Eq. 3) was derived from observations collected at the peak of the 2016 marine heatwave (Hughes et al. 2018). The response of corals to thermal stress over 6 months (i.e., initial + post-bleaching mortality) was determined by calibration with the observed coral cover changes (n = 63) sampled 8 months after the survey of initial mortality of the 2016 GBR bleaching (Hughes et al. 2018). We simulated 63 hypothetical reefs with a pre-bleaching coral cover generated at random from the frequency distribution observed in March 2016 dis-aggregated per coral type, assuming 50% acroporids. The modeled reefs were then randomly subjected to the reported DHW values (n = 63 DHW estimates). For each thermal stress above 3 DHW (threshold of significant mortality during the 2016 heatwave, Hughes et al. 2018), a stochastic estimate of $M_{BleachInit}$ was predicted (main text Eq. 3) with a Gaussian random noise. Extending $M_{BleachInit}$ to 6 times the period over which initial mortality was recorded (i.e., $1 - (1 - M_{BleachInit} / 100)^6$) allowed to reproduce the observed changes in coral cover 8 months after bleaching (main text, Figs. 2D-E).

GBR observations of coral cover

The benthic survey database of the Australian Institute of Marine Science (Sweatman et al. 2008, Thompson et al. 2019) was used (1) to calibrate cyclone-driven coral mortality, (2) to initialize the 2008–2020 reconstruction of reef trajectories with realistic reef-level coral cover and (3) to validate this reconstruction.

On mid-shelf and outer reefs, monitoring surveys followed two protocols (Sweatman et al. 2008, Miller et al. 2009): (1) permanent photo transects, conducted at 6–9 m depth on three sites on the northeast flank of a reef and providing a fine-scale assessment of multiple coral taxa; (2) manta tows, conducted over the entire perimeter of a reef by a towed snorkel diver and providing a rapid assessment of coral cover on a categorical scale. Data on inshore reef (Thompson et al. 2019) were obtained from permanent photo transects conducted at 5 m depth at each of two sites. Although the two methods produce similar assessments when applied to the same reef portion (Miller and Müller 1999), reef-wide coral cover estimates from manta tows tend to be lower due to the inclusion of non-coral habitats in the tow path (Osborne et al. 2011, Sweatman and Syms 2011). These biases were minimized by converting manta-tow cover estimates into a transect equivalent from the linear regression of 1992–2018 joint estimates from the same reef and year (R^2 = 0.53, n = 893 joint observations):

$$\%C_{transect} = 7.2 + 0.9 \times \%C_{tow} \quad \text{(S15)}$$

Model performance

Model predictions of total coral cover were compared to time-series from the AIMS reef benthic database (transects and standardized manta tows). We selected $n = 95$ individual reefs monitored at least 6 times between 2009–2020 (i.e., excluding the pre-2009 surveys that were used for model initialization). For each reef, we visually compared the mean coral cover value predicted by the model and the mean observed coral cover of the corresponding season/year (Fig. S17). We also calculated the deviations between individual predictions and the mean observed coral cover (i.e., prediction errors) and compared them with the deviations between individual observations and their mean value (observation errors) to account for the within-reef variability associated to monitoring data. The reason is because coral cover observations exhibited important variability among sites of the same reef, making the use of a reef-wide mean cover inappropriate to assess the match with model predictions.

While 40 model predictions of coral cover are systematically available on a given reef at a given time step, observations are only represented by 2 or 3 mean cover estimates derived from permanent photo transects, and/or one derived from manta tows (standardized to an equivalent transect). For each observed time t, we randomly sampled 40 estimates of coral cover from normal distributions with means μ_t equal to the overall mean coral cover at t and the associated standard error ($n = 2$, 3 or 4). When only one cover estimate was available (i.e., from manta tows), we randomly generated 40 transect-equivalent cover estimates from the linear model (Eq. S15) with a Gaussian error of mean equal to zero and variance equal to the estimated error variance of the model. As a result, coral cover predictions ($y_{j,t}$) and re-sampled 'observations' ($x_{i,t}$) at any observed time t have equal sample size ($n = 40$) which allows calculation of errors in coral cover prediction ($y_{j,t} - \mu_t$) and observation ($x_{i,t} - \mu_t$) as deviations from the population mean. We determined the 90% error interval of each distribution defined as the range between the 5th and 95th percentiles, and visually assessed their overlap for the 95 select reefs (Fig. S18).

Overlapping error intervals tend to indicate a good match between predicted and observed coral cover over time (compare Figs. S17 and S18), while departures of the predicted error interval towards positive or negative errors tend to indicate, respectively, over-prediction or under-prediction of the observed distribution of coral cover values. The greater the departure, the greater the difference between predictions and observations, either at a particular point of time or throughout the available time series.

A number of caveats pertain to the evaluation of model performance against monitoring data, regardless of the method chosen for assessing the match between predicted and observed coral cover. First, many model errors were due to the erroneous prediction of reef exposure to cyclone intensity. While this constitutes an error in the forcing spatial layers, this does not invalidate the modeling of underlying coral demographics. Yet, an erroneous prediction of cyclone exposure

occurring early in the reconstruction (e.g., Cyclone Hamish in 2009) generates a substantial prediction error that is carried over the entire timeframe; this has considerable influence on the overall distribution of prediction errors, even if the coral dynamics after disturbance were well reproduced by the model. Second, observations were assigned to the corresponding time step of the model based on the dates of the monitoring surveys, yet some reefs were surveyed just *before* the aftermath of an acute disturbance while being assigned to the time step of the disturbance event; this creates considerable departures between predictions and observations, even though the prediction was correct within a few months.

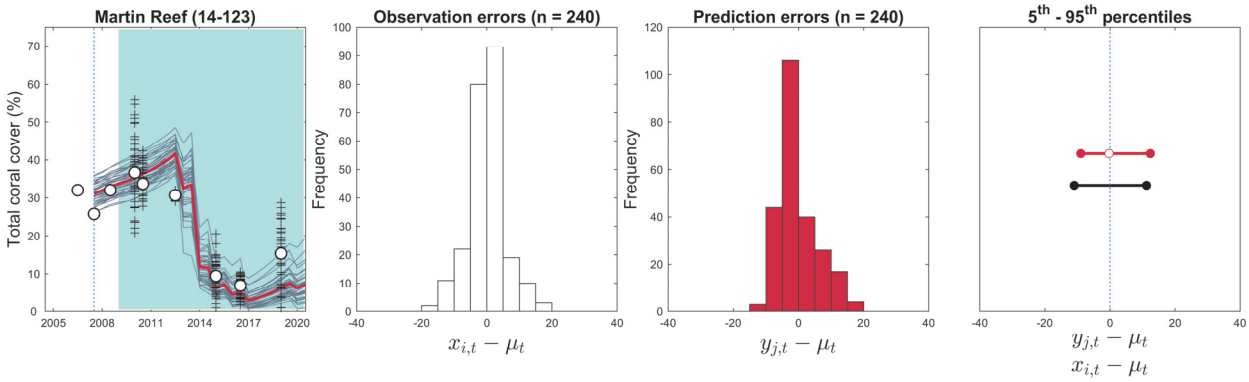

Fig. S2. Graphical example of calculation of model prediction and observation errors from the reconstructed trajectories of coral cover (grey lines: individual trajectories, $n = 40$; red line: average trajectory) and LTMP observations (open circles: overall mean coral cover μ_t at time t from permanent transects and/or standardized manta tows). For each observed time after 2009 (blue zone), 40 'observations' (plus signs) are generated at random to balance the distribution of predicted coral cover values. Here (Martin Reef, inshore northern GBR), monitoring observations were available for 6 time steps, generating a global distribution of 240 observation errors (white bars) over the monitored period, and a corresponding distribution of 240 prediction errors (red bars). Each error distribution can be summarized by a 90% error interval, defined as the range between the 5th and 95th percentiles (open circle: mean prediction error).

References

Arnold, S. N., R. S. Steneck, and P. J. Mumby. 2010. Running the gauntlet: inhibitory effects of algal turfs on the processes of coral recruitment. Marine Ecology Progress Series 414:91–105.

Baird, A., and P. Marshall. 2002. Mortality, growth and reproduction in scleractinian corals following bleaching on the Great Barrier Reef. Marine Ecology Progress Series 237:133–141.

Box, S. J., and P. J. Mumby. 2007. Effect of macroalgal competition on growth and survival of juvenile Caribbean corals. Marine Ecology Progress Series 342:139–149.

Bozec, Y.-M., L. Alvarez-Filip, and P. J. Mumby. 2015. The dynamics of architectural complexity on coral reefs under climate change. Global Change Biology 21:223–235.

Bozec, Y.-M., C. Doropoulos, G. Roff, and P. J. Mumby. 2019. Transient grazing and the dynamics of an unanticipated coral–algal phase shift. Ecosystems 22:296–311.

Bozec, Y.-M., S. O'Farrell, J. H. Bruggemann, B. E. Luckhurst, and P. J. Mumby. 2016. Tradeoffs between fisheries harvest and the resilience of coral reefs. Proceedings of the National Academy of Sciences 113:4536–4541.

Bythell, J. C., E. H. Gladfelter, and M. Bythell. 1993. Chronic and catastrophic natural mortality of three common Caribbean reef corals. Coral Reefs 12:143–152.

Carrigan, A. D., and M. Puotinen. 2014. Tropical cyclone cooling combats region-wide coral bleaching. Global Change Biology 20:1604–1613.

De Ruyter van Steveninck, E. D., and A. M. Breeman. 1987. Deep water populations of Lobophora variegata (Phaeophyceae) on the coral reef of Curaçao: influence of grazing and dispersal on distribution patterns. Marine Ecology Progress Series 38:241–250.

De Ruyter van Steveninck, E. D., L. L. Van Mulekom, and A. M. Breeman. 1988. Growth inhibition of Lobophora variegata (Lamouroux) Womersley by scleractinian corals. Journal of Experimental Marine Biology and Ecology 115:169–178.

Diaz-Pulido, G., and L. J. McCook. 2004. Effects of live coral, epilithic algal communities and substrate type on algal recruitment. Coral Reefs 23:225–233.

Doropoulos, C., G. Roff, Y.-M. Bozec, M. Zupan, J. Werminghausen, and P. J. Mumby. 2016. Characterizing the ecological trade–offs throughout the early ontogeny of coral recruitment. Ecological Monographs 86:20–44.

Doropoulos, C., S. Ward, G. Roff, M. González-Rivero, and P. J. Mumby. 2015. Linking demographic processes of juvenile corals to benthic recovery trajectories in two common reef habitats. PLoS ONE 10:e0128535.

Edwards, H. J., I. A. Elliott, C. M. Eakin, A. Irikawa, J. S. Madin, M. McField, J. A. Morgan, R. van Woesik, and P. J. Mumby. 2011. How much time can herbivore protection buy for coral reefs under realistic regimes of hurricanes and coral bleaching? Global Change Biology 17:2033–2048.

Hall, V., and T. Hughes. 1996. Reproductive strategies of modular organisms: comparative studies of reef-building corals. Ecology 77:950–963.

Hughes, T. P., J. T. Kerry, A. H. Baird, S. R. Connolly, A. Dietzel, C. M. Eakin, S. F. Heron, A. S. Hoey, M. O. Hoogenboom, G. Liu, and others. 2018. Global warming transforms coral reef assemblages. Nature 556:492.

Humanes, A., G. F. Ricardo, B. L. Willis, K. E. Fabricius, and A. P. Negri. 2017a. Cumulative effects of suspended sediments, organic nutrients and temperature stress on early life history stages of the coral Acropora tenuis. Scientific Reports 7:44101.

Humanes, A., A. Fink, B. L. Willis, K. E. Fabricius, D. de Beer, and A. P. Negri. 2017b. Effects of suspended sediments and nutrient enrichment on juvenile corals. Marine Pollution Bulletin 125:166–175.

Jompa, J., and L. J. McCook. 2002a. The effects of nutrients and herbivory on competition between a hard coral (*Porites cylindrica*) and a brown alga (*Lobophora variegata*). Limnology and Oceanography 47:527–534.

Jompa, J., and L. J. McCook. 2002b. Effects of competition and herbivory on interactions between a hard coral and a brown alga. Journal of Experimental Marine Biology and Ecology 271:25–39.

Kuffner, I. B., L. J. Walters, M. A. Becerro, V. J. Paul, R. Ritson-Williams, and K. S. Beach. 2006. Inhibition of coral recruitment by macroalgae and cyanobacteria. Marine Ecology Progress Series 323:107–117.

Lenihan, H. S., S. J. Holbrook, R. J. Schmitt, and A. J. Brooks. 2011. Influence of corallivory, competition, and habitat structure on coral community shifts. Ecology 92:1959–1971.

Lirman, D. 2001. Competition between macroalgae and corals: effects of herbivore exclusion and increased algal biomass on coral survivorship and growth. Coral Reefs 19:392–399.

Liu, G., W. J. Skirving, E. F. Geiger, J. L. De La Cour, B. L. Marsh, S. F. Heron, K. V. Tirak, A. E. Strong, and C. M. Eakin. 2017. NOAA Coral Reef Watch's 5km satellite coral bleaching heat stress monitoring product suite version 3 and four-month outlook version 4. Reef Encounter 32:39–45.

Madin, J. S., and S. R. Connolly. 2006. Ecological consequences of major hydrodynamic disturbances on coral reefs. Nature 444:477–480.

Massel, S. R., and T. J. Done. 1993. Effects of cyclone waves on massive coral assemblages on the Great Barrier Reef: meteorology, hydrodynamics and demography. Coral Reefs 12:153–166.

Manzello, D. P., Brandt, M., Smith, T. B., Lirman, D., Hendee, J. C., and R. S. Nemeth. 2007. Hurricanes benefit bleached corals. Proceedings of the National Academy of Sciences, 104:12035–12039.

Meesters, E. H., M. Hilterman, E. Kardinaal, M. Keetman, M. deVries, and R. P. M. Bak. 2001. Colony size-frequency distributions of scleractinian coral populations: spatial and interspecific variation. Marine Ecology Progress Series 209:43–54.

Meesters, E. H., I. Wesseling, and R. P. Bak. 1997. Coral colony tissue damage in six species of reef-building corals: partial mortality in relation with depth and surface area. Journal of Sea Research 37:131–144.

Miller, I., M. Jonker, and G. Coleman. 2009. Crown-of-thorns starfish and coral surveys using the manta tow and SCUBA search techniques. Australian Institute of Marine Science, Townsville, Australia.

Miller, I., and R. Müller. 1999. Validity and reproducibility of benthic cover estimates made during broadscale surveys of coral reefs by manta tow. Coral Reefs 18:353–356.

Mumby, P. J. 1999. Bleaching and hurricane disturbances to populations of coral recruits in Belize. Marine Ecology Progress Series 190:27–35.

Mumby, P. J., N. L. Foster, and E. A. G. Fahy. 2005. Patch dynamics of coral reef macroalgae under chronic and acute disturbance. Coral Reefs 24:681–692.

Mumby, P. J., A. Hastings, and H. J. Edwards. 2007. Thresholds and the resilience of Caribbean coral reefs. Nature 450:98–101.

Mumby, P. J., N. H. Wolff, Y.-M. Bozec, I. Chollett, and P. Halloran. 2014. Operationalizing the resilience of coral reefs in an era of climate change. Conservation Letters 7:176–187.

Nugues, M. M., and R. P. Bak. 2006. Differential competitive abilities between Caribbean coral species and a brown alga: a year of experiments and a long-term perspective. Marine Ecology Progress Series 315:75–86.

Ortiz, J. C., Y.-M. Bozec, N. H. Wolff, C. Doropoulos, and P. J. Mumby. 2014. Global disparity in the ecological benefits of reducing carbon emissions for coral reefs. Nature Climate Change 4:1090.

Osborne, K., A. M. Dolman, S. C. Burgess, and K. A. Johns. 2011. Disturbance and the dynamics of coral cover on the Great Barrier Reef (1995–2009). PLoS ONE 6:e17516.

Puotinen, M., J. A. Maynard, R. Beeden, B. Radford, and G. J. Williams. 2016. A robust operational model for predicting where tropical cyclone waves damage coral reefs. Scientific Reports 6:26009.

Sweatman, H. H., A. A. Cheal, G. G. Coleman, M. M. Emslie, K. K. Johns, M. M. Jonker, I. I. Miller, and K. K. Osborne. 2008. Long-term Monitoring of the Great Barrier reef, Status Report 8. Australian Institute of Marine Science, Townsville, Australia.

Sweatman, H., and C. Syms. 2011. Assessing loss of coral cover on the Great Barrier Reef: A response to Hughes et al.(2011). Coral Reefs 30:661.

Thompson, A., P. Costello, J. Davidson, M. Logan, and G. Coleman. 2019. Marine Monitoring Program: Annual report for inshore coral reef monitoring 2017-18.

Wallace, C. 1999. Staghorn corals of the world: a revision of the genus Acropora. CSIRO publishing.

Williams, I. D., N. V. Polunin, and V. J. Hendrick. 2001. Limits to grazing by herbivorous fishes and the impact of low coral cover on macroalgal abundance on a coral reef in Belize. Marine Ecology Progress Series 222:187–196.

Zhang, H., He, H., Zhang, W. Z., and D. Tian. 2021. Upper ocean response to tropical cyclones: a review. Geoscience Letters 8:1–12.